Proceeding of the IEEE
International Conference on Robotics and Biomimetics
Dali, China, December 2019

Task-Oriented Design Optimization for a Mobile Painting Robot*

Ye Ma and Ning Xi
Department of Industrial and Manufacturing Systems Engineering
The University of Hong Kong
Hong Kong SAR, China
{u3004939 & xining}@connect.hku.hk

Sheng Bi
Shenzhen Academy of Robotics
Shenzhen, 518000, China
bisheng@szarobots.com

***Abstract* - Under the specific task requirement of mobile manipulators, the workspace analysis plays an indispensable role in the design and optimization of their geometric structure. To generate the most suitable workspace for mobile manipulators and cater to specific task requirement, the geometric structure parameter of mobile manipulators should be optimized and this need to consider the effective information from operated target. When deal with one specific operating task by painting one prototype room composed of vertical plane walls and ceilings, this research presents one novel method for designing and optimizing the structure parameter of mobile painting robot. To be specific, the feature extraction is executed for the operated target-prototype room, and the corresponding feature constraints function is established. Closely following this, under the given optimized goals, the optimized structure parameter of the mobile painting robot for specific operation will be obtained. What's more, to verify the validation of obtained structure parameter, the painting simulation platform via V-REP software is established, and the painting path which is attached with painting effect for painting the whole prototype room is analyzed initially. Last but not least, the smooth implementation of simulation process demonstrates that the optimized structure parameter can fulfill the task requirement, and this has actually confirmed one feasible way of task-oriented structure optimization for mobile painting robot.**

Index Terms* - *workspace analysis; optimization design; mobile painting robot; painting thickness distribution.

I. INTRODUCTION

Specifically, the utilization of spray painting in industry can be traced to the industry development in early days, and it aims to improve original operation quality, accuracy, and efficiency by replacing the conventional manual operations. It is widely acknowledged that the current spray paint operation has been widely applied in these industrial areas such as construction, aircraft, automobiles and control. Also the trend for painting system is to try to pursue higher self-determination, flexibility and rate of safety in the future [1]. Under this situation, the automatic painting robotic system is adopted by many commercial robotic companies, such as ABB, KUKA, with manufactured multi DOF (degree of freedom) industrial robot which is designed for specific tasks [2]. Moreover, the research for painting robot has been conducted during past few years, and it pays more attention to the painting mechanism and structure (pneumatic nozzles, air brush and spray gun) [3], the optimal trajectory planning for the whole system [4][5], and the painting materials thickness distribution [6] which can guarantee the quality requirement with given task constraints. In order to satisfy various working environment, the painting robot can be classified via indoor robot [7] which usually owns one fixed/mobile platform to deal with interior work piece and outdoor robot [8][9] which adopts suspension system to support the robot base. Therefore, it is certain to say that the issue for the design and optimization of a painting robot is significantly important.

Besides, the existed design and optimization for painting robot are usually "self-centered". In other words, the design mainly focuses on the improvement for the self-performance of partial assembly but not just to consider one specific operation tasks from one macro perspective. It can be justified without any exaggeration that very little effective information from the operated target is considered and involved during the design and optimization process. Under this situation, the "waste phenomenon" and low utilization rate for the performance from designed structure is inevitable. For example, according to Fig.1 (a), the workspace of robot shows a huge occupying space yet very little utilization rate. But according to Fig. 1 (b), the workspace not only shows one higher utilization rate but with one similar shape compared to operating target. Based on these information, we could conclude that the workspace from Fig.1 (b) exhibits better performance than the workspace from Fig.1 (a). In fact, the workspace of the painting robot fundamentally determines the painting quality during painting operation, painting trajectory, as well as painting material distribution process. It is really necessary and imperative to say that the optimization for workspace of painting robot which can cater to specific operation tasks should be further considered. However, two important issues have arisen. The first one is about the workspace optimization for painting robot. Due to that the workspace is determined by the geometric structure of painting manipulator (painting arm), and the design and optimization process actually focus on the structure parameter of painting manipulator, herein the D-H (Denavit-Hartenberg) parameters was adopted [10]. The

* This research was partially supported by Shenzhen Basic Research Projects Foundation (JCYJ 20160429161539298), Shenzhen Overseas High Level Talent (Peacock Plan) Program (KQTD20140630154026047), and Gammon Construction Limited, Hong Kong.

978-1-7281-6321-5/19//$31.00 ©2019 IEEE

second one is about how to obtain the effective information from one specific operation task in terms of optimized workspace. That is to say, it is about how to use the mathematical language to describe one specific operation target, and herein one "feature point" extraction method with establishing the feature point constraints function was introduced.

(a) Inferior performance

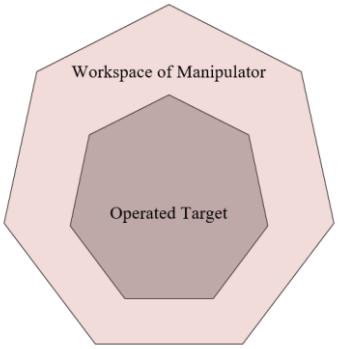

(b) Superior performance

Fig. 1 The comparison for the performance of manipulator's workspace

The research focuses on designing the structure parameter for painting manipulator from one mobile painting robot which can cater to one specific operating task. The initial model for the painting manipulator is inspired by SCARA Robot [11] which pays attention to the plane or assembly operations, and the mature commercial product Husky UGV. Here, it is noted that high flexibility and pay-load performance are adopted as the mobile platform. To be exact, we choose the whole prototype room as the painting target, with 40 m^2 built-up area, 2.4m height, and it is composed of 5 vertical planar walls and 2 ceilings. From the details for the structure optimization for multi-DOF manipulator, the structure synthesis as well as the dimensional synthesis [12] was involved, and the corresponding optimization function which includes optimized parameter, goal, algorithm and constraints can be collected and established as well. To verify the final painting quality, the optimization method for the painting path [13][14] and the painting thickness distribution model [10] were adopted during simulation process. The simulation platform was established via V-REP software and data processing and analysis process were completed via MATLAB software. The key contents can be summarized in the following several parts. In part II, it mainly illustrated the theoretical knowledge which is employed in this research, such as the kinematics of mobile painting robot, feature point extraction method for operated target, modeling of painting thickness distribution and optimization function establishment. In part III, the feature point for the operated target was extracted and the optimization results for structure parameters were obtained via Monte-Carlo algorithm. All of these were verified by painting the whole prototype room in V-REP based simulation platform. In part IV, it shows the detailed information about both conclusion and future plans.

II. MODELLING AND OPTIMIZATION METHODS

In order to obtain the optimal geometric structure of mobile painting robot, it is really necessary and imperative to conduct the performance analysis for the painting robot's structure and the feature extraction from operated target. During this process, the following contents are involved, such as the fundamental studies of kinematics of mobile painting robotic system, the mathematical model of painting thickness distribution as well as the establishment of optimization function.

A. Kinematics of Mobile Painting Robot

Specifically, the kinematics of the whole system are accommodated and the main purpose is to obtain the detailed expressions of workspace for mobile painting robot. Moreover, it mainly restricts the reachable space for end-effector, namely the spray gun, and can be employed to inverse resolve the desired joint trajectory based on desired painting path generated from painting requirement. We can define the world coordinate frame by Σ_w; the fixed coordinate frame Σ_b for mobile platform, Σ_i for joint i and Σ_n for end-effector, and T_{i-1}^{i} as the D-H conversion matrix from (i-1)th fixed frame to ith fixed frame. According to D-H parameter description method, the signal a_i and a_n denote the length of link i and end-effector, respectively; the signal θ_i or q_i (Generalized form) as the angle of joint i, the α_i as the twist angle of link i, and the d_i as the offset of link i; the generalized variable q_i as the angle of joint i (i=1,…,n) and as the posture information of mobile platform (i=0).

Therefore, we have the D-H matrix as:

$$T_{i-1}^{i}=\begin{bmatrix} \cos(\theta_i) & -\sin(\theta_i) & 0 & \alpha_{i-1} \\ \sin(\theta_i)\cos(\alpha_{i-1}) & \cos(\theta_i)\cos(\alpha_{i-1}) & -\sin(\alpha_{i-1}) & -\sin(\alpha_{i-1})d_i \\ \sin(\theta_i)\sin(\alpha_{i-1}) & \cos(\theta_i)\sin(\alpha_{i-1}) & \cos(\alpha_{i-1}) & \cos(\alpha_{i-1})d_i \\ 0 & 0 & 0 & 1 \end{bmatrix} \quad (1)$$

$$\begin{aligned} T_0^n &= T_0^b(q_0)T_b^1(q_1)T_1^2(q_2)T_2^3(q_3)\cdots T_{n-1}^n(q_n) \\ &= \begin{bmatrix} R_0^n & P_0^n \\ 0\ \ 0\ \ 0 & 1 \end{bmatrix} \end{aligned} \quad (2)$$

in which R_0^n denotes the rotation transformation from Σ_w to Σ_n, and P_0^n denotes the corresponding position transformation. And therefore, the position and orientation transformation relationship from world coordinate frame to the fixed frame of

end-effector (spray gun) can be obtained, with the given q_i (Generalized form). So, (2) can offer the detailed expressions of absolute coordinate for the end-effector, that is, the reachable space for the spray gun, by which the Jacobian matrix and the boundary of workspace Ψ_i (μ_i) can be derived as well.

B. *Extraction for Feature Point*

When the task point space from operated target incorporates infinite elements, it is quite difficult to deal with the point set with infinite data by employing conventional analytical or numerical methods. This problem can be effectively solved by extracting the limited representative characteristics, for example, points or segments from operating targets which can stand for the whole task point space. However, the characteristics mentioned here have a close relationship with the workspace of manipulator rather than the inertial coordinate frame. Under this situation, the extraction process for effective feature point of one specific workspace can be shown in Fig. 2.

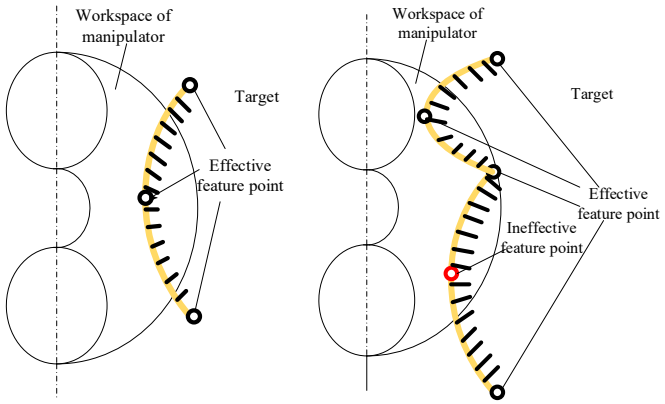

Fig. 2 Identification for the effective "feature point"

According to the information in Fig.2, we can conclude that the feature point which is related to one specific workspace is the "farthest" and "nearest" point to the workspace. To specify these feature points from operated target and determine the boundary point of workspace, the determinant expression from (2) is required.

$$\boldsymbol{F}_{\max}=\max|\boldsymbol{f}-\Psi^{i}(\mu_i)| \tag{3}$$

$$\boldsymbol{F}_{\min}=\min|\boldsymbol{f}-\Psi^{i}(\mu_i)| \tag{4}$$

Now, we assume that the CAD (computer aided design) modeling of the operated target can be denoted by $\boldsymbol{f}$. So it is correct to say that the "farthest" and "nearest" point can be defined by (3) to (4) respectively, in which $\boldsymbol{F}_{\max}$ or $\boldsymbol{F}_{\min}$ is one set of point.

C. *Modeling of Painting Thickness Distribution*

This research has adopted the painting deposition model with the form of parabolic model [15] to deduce the painting thickness in theory. Due to the various painting requirement for painting thickness, and the painting deposition model as well as the task requirement determines the allowable motion range for one specific spray gun model. Therefore, the spray gun model and its allowable motion curves should be specified, attached with the maximum and minimum range of painting thickness. The painting zone of one specific spray gun model can be simplified by one circular cone, shown in Fig. 3(a).

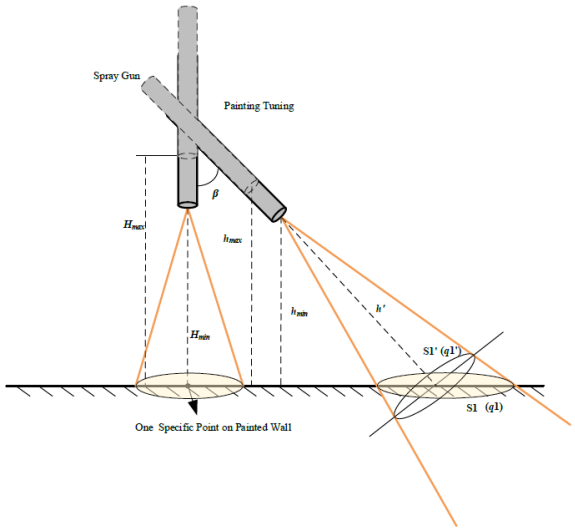

(a) Spray gun mathematical model

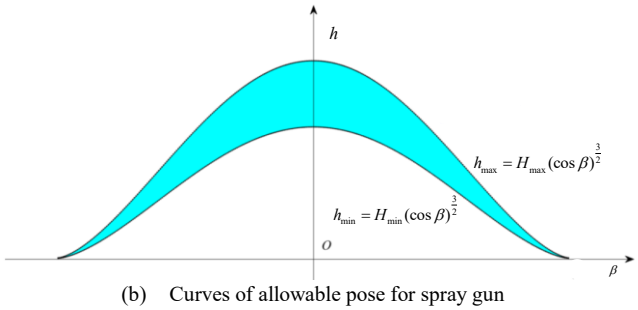

(b) Curves of allowable pose for spray gun

Fig. 3 Modeling of painting tool

From Fig.3 (a), we define the desired quantity painted on the plane wall as $\boldsymbol{q}_d$, and maximum and minimum allowable quantity as $\boldsymbol{q}_{\max}$, $\boldsymbol{q}_{\min}$. The desired maximum and minimum painting height when the painting direction is perpendicular to the plane wall are $\boldsymbol{H}_d$, $\boldsymbol{H}_{min}$ and $\boldsymbol{H}_{\max}$, respectively. Therefore, the relationship shown as follows can be obtained:

$$\left(\frac{H_d}{H_{\min}}\right)^2=\frac{q_{\max}}{q_d} \tag{5}$$

$$\left(\frac{H_d}{H_{\max}}\right)^2=\frac{q_{\min}}{q_d}$$

where,

$$H_{\min}=H_d\sqrt{\frac{q_d}{q_{\max}}} \tag{6}$$

$$H_{\max}=H_d\sqrt{\frac{q_d}{q_{\min}}}$$

When the spray gun rotates with angle β, the maximum and minimum painting height will be changed to $h_{\max}$, $h_{\min}$, and we can obtain the relationships as follows:

$$q_1 = q_1' \cdot \cos(\beta) \tag{7}$$
$$q_{\min} \le q_1 \le q_{\max}$$
$$\frac{q_{\min}}{\cos(\beta)} \le q_1' \le \frac{q_{\max}}{\cos(\beta)}$$

So, the h' can be obtained by:

$$h'_{\max} = H_{\max}\sqrt{\cos(\beta)} \tag{8}$$
$$h'_{\min} = H_{\min}\sqrt{\cos(\beta)}$$

Therefore,

$$h_{\max} = h'_{\max}\cos(\beta) = H_{\max}(\cos(\beta))^{3/2} \tag{9}$$
$$h_{\min} = h'_{\min}\cos(\beta) = H_{\min}(\cos(\beta))^{3/2}$$

And thereby we can obtain the function of allowable painting height with variable β, shown as Fig.3 (b):

In Fig.3(b), $\beta \in (-\pi/2, \pi/2)$, and the light blue area in figure shows the available workspace for spray gun which can fulfill the painting quantity requirement. Based on the spray gun mathematical model which is showed in Fig.3 (b), we can derive the allowable motion range of spray gun (one specific point) in inertial frame.

D. Optimization Function Establishment

The optimization process can be summarized as follows: extracting the effective feature points from operated target; define the optimized parameter for manipulator (D-H parameters); determine the optimized index, constraints, algorithm; verification.

1) Optimized Parameter: the optimization design can be classified by both the structure synthesis and dimensional synthesis. To be specific, the structure synthesis focuses on the adjustment of joint number and joint installation orientation, but the dimensional synthesis involves in the length of each link, the twist angle and other D-H parameters. Moreover, the structure synthesis mainly considers the minimum allowable amount for installed joint, and simultaneously it can guarantee the accomplishment of task requirement. Therefore, the structure synthesis mainly focuses on the amount for painting manipulator so as to satisfy the position/orientation requirement. However, as to the dimensional synthesis, the D-H parameters of painting arm are considered as the optimized parameters, and a consequential increase can be found in optimized parameter set with the increase of revolute joint.

2) Optimized Index: several typical indices in existed studies are briefly illustrated, for example, the structural length, manipulability and condition number.

The structural length tends to pursue the highest cost-effective value for the total link length and the volume of workspace. Generally speaking, a "longer" manipulator owns one larger reachable workspace. However, the robot manipulators with the same link length owns different reachable work-spaces, this is actually a unique phenomenon. By taking the given value of total link length into consideration, it is easy to find that the one with larger workspace would indicate one better performance for its structure parameters. Based on the structural length, it is predicted that the excellent structure design would exhibit one small link length sum but with a large workspace volume.

The condition number of the Jacobian matrix is used to estimate the error and the accuracy of the Cartesian velocity of the end-effector in its reachable workspace.

The index of manipulability was proposed to indicate the dexterity of each point of workspace that is generated from the manipulator. Two expression forms for the index can be found when considering the condition that if the Jacobian matrix of manipulator is a non-homogeneous matrix.

3) Constraints: the constraints can be divided into the following two categories. The first one is the feature constraints function that is generated from extracted feature points of operated target. This can be defined by (10), in which $\boldsymbol{f}$ the forward kinematics and the allowable threshold, the $\boldsymbol{F}(i) = \{\boldsymbol{F}_{\max}, \boldsymbol{F}_{\min}\}$ the coordinates of effective feature points from operated target. The second one is the physical constraints, such as the obstacle avoidance and the distance interval of mobile. They are regarded as the platform to operated target and the allowable motion range of spray gun.

$$\exists\theta \in (\theta_{\min}, \theta_{\max}), Constraints: \ \|f(a,\alpha,d,\theta) - F(i)\| \le \varepsilon \tag{10}$$

4) Optimized Algorithm: the Monte Carlo method [16] is applied to surf the global optimal solution. The one need to be mentioned is that this method is in the form of random sampling on the whole feasible zone. Here, with the specific feature constraints function attached with other physical constraints and requirement, the feasible zone for the structure parameter is determined. Moreover, a large number of discrete points are required for the purpose of getting good results in the proposed method.

III. Simulation and Analysis

Herein, we adopted the model of prototype room, shown in Fig. 4(a), (5 vertical walls and two ceilings to be painted) as the specific operated target. Based on (3)-(4) we extracted the feature point from the prototype room, with considering all the corners and turning of walls or windows congruent with the "farthest" and "nearest" point to the workspace. Totally, there exists 22 points extracted from prototype room, shown in Fig.4(b), generated via MATLAB.

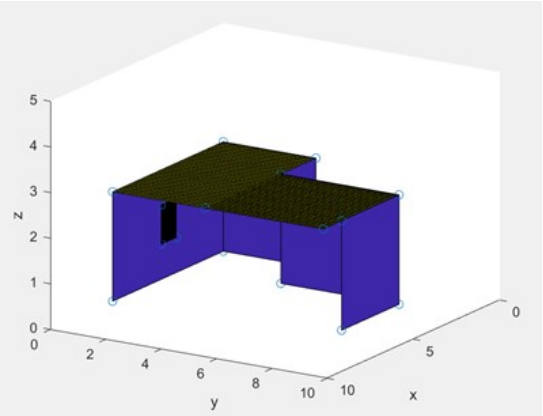

(a) Model of prototype room

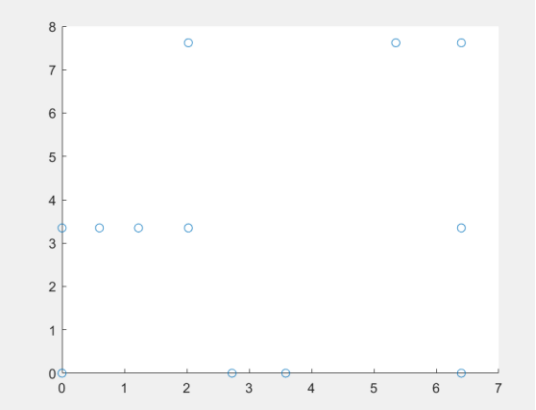

(b) Feature point distribution (top view)

Fig. 4 Feature point extraction from model of prototype room

So based on the coordinates of all the feature points, the feature constraints function can be replaced via (11).

$$\text{Constraints}: \left\| \boldsymbol{f} - \boldsymbol{F}_m \right\| \le \tau, m = 1,...,22 \tag{11}$$

in which $\boldsymbol{f}$ denotes the forward-kinematics of painting arm, and $\boldsymbol{F}_{\mathrm{m}}$ denotes the vector of target point m (position, orientation) on the surface of operated target.

1) Structure Synthesis: We choose the joint number that can fulfill all the constraints function (11) as the optimized parameter, and from the initial model of painting manipulator inspired from SCARA, more than 3 revolute joints as well as one translational joint will be involved, so (12) can be replaced via (12), and based on the Monte Carlo solution process, we can initially conclude that the minimum joint number is 5 (1 translational joint as well as 4 revolute joints).

$$\begin{aligned} &\exists \theta_i \in (\theta_{\min}, \theta_{\max}), d_1 \in (d_{\min}, d_{\max})\ i = 2,... \\ &s.t.\ \left\| \boldsymbol{f}(S, \theta_i, d_1) - F_m \right\| \le \tau \\ &S: a_0, \alpha_0, \theta_1; a_1, \alpha_1, d_2; a_2, \alpha_2, d_3; a_3, \alpha_3, d_4 ... \end{aligned} \tag{12}$$

2) Dimensional Synthesis: the set S in (12), shows the optimized parameters, mainly the D-H parameters including the link length, offset and twist angle. So based on the minimum joint configuration, set S can be replaced via S^* (13).

$$S^*: a_0, \alpha_0, \theta_1; a_1, \alpha_1, d_2; a_2, \alpha_2, d_3; a_3, \alpha_3, d_4; a_4, \alpha_4, d_5 \tag{13}$$

Now we randomly select 1000,000 discrete points for each dependent parameter ($d_1, \theta_2, \theta_3, \theta_4, \theta_5$), and according to the actual working condition we the set θ_1=0 and other feasible space of S^* as follows:

$$\begin{aligned} &\alpha_i = \frac{n\pi}{2}, n \in \{-2,-1,0,1,2\} \\ &a_i \in (0,2)\ i = 2,...,5 \\ &d_i \in (-2,2), i = 2,...,5 \end{aligned} \tag{14}$$

Then we randomly selected 10,000 groups of discrete points on the space of S^*, and obtained 1898 points that fulfill the constraints of (13) and other physical constraints. And based on the optimized indices mentioned in II, we can obtain the corresponding optimal parameter configuration from the 1892 group parameters, shown in Fig.5, in which a larger value would indicate one better performance. In Fig. 6, the comprehensive index was considered, from which we choose one group of parameter configuration with good performance (unified homogenization index≈1.38, with superior overall and local performance) as one detailed example to verify the painting effect, with a_0=0(m); a_1=0.087(m); a_2=0.251(m); a_3=0.01(m); a_4=0.242(m); d_2=-0.001; d_3=-0.023; d_4=0.064; d_5=0.002; α_0=0; α_1=0; α_2=0(rad); α_3=-π/2(rad); α_4=0(rad).

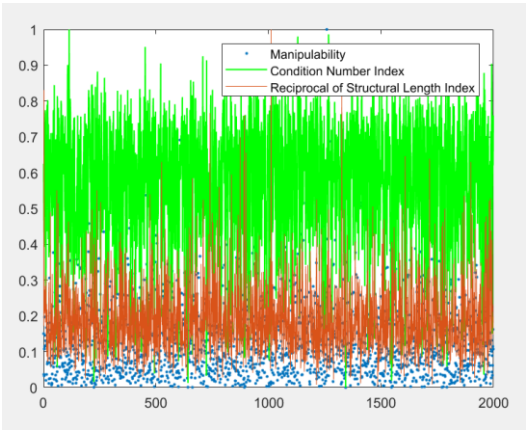

Fig.5 Various optimized index (manipulability; condition number; structural length)

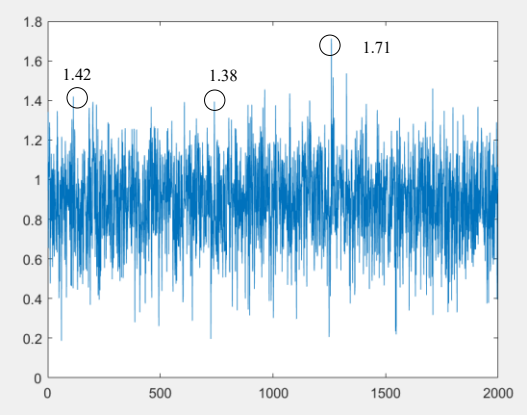

Fig. 6 Unified homogenization index (manipulability+condition number+reciprocal of structural length)

We established a V-REP simulation platform to finish the painting operation for the whole house. Based on [15], the desired painting path can be obtained and was shown in Fig. 7.

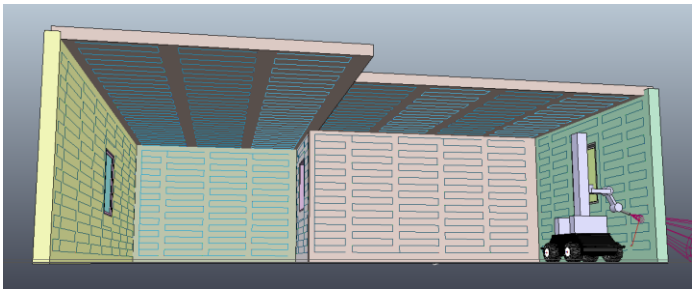

Fig. 7 Desired painting path in V-REP simulation platform

Now we chose optimized configuration mentioned above to set up the painting manipulator, and model of Husky UGV as the mobile platform. The painting deposition model proposed in [15] was adopted here, and the corresponding

painting effect can be detected and analyzed in theory. The simulation process can be shown in Fig. 8.

From Fig. 8, the complete painting process was started from vertical wall to the ceiling, and based on the V-REP software path tracing error alarm function, the desired painting path can be guaranteed with proper structure parameter from painting manipulator and effective painting path planning. The desired trajectory for each joint of painting manipulator can be derived via inverse-kinematics of the system. And at this stage, the motion path of mobile platform can be properly selected within the workspace of itself. We set the painting requirement $\boldsymbol{q}_{max}$=1.25 $\boldsymbol{q}_{d}$, and $\boldsymbol{q}_{min}$=0.75 $\boldsymbol{q}_{d}$ ($\boldsymbol{q}_{d}$ denotes the desired painting quantity) and with the initial measure from visual detection function of V-REP software, the painting thickness distribution results can be shown in TABLE I, which confirmed the effectiveness and feasibility of the painting process.

Therefore, compared with previous studies, our optimized painting robotic system exhibits compacter geometric structure as well as shorter structural length under the premise of ensuring the painting precision. In addition, we try to decrease the number of the joints installed on the painting manipulator in order to reduce the cost, which is different from the system directly adopting the commercial product. Herein, the comprehensive optimization index was employed in case of weakness performance for single index. The painted target model - prototype room contains actual corners, turnings ceiling and windows, which makes the proposed method more convincing for the future painting experiment. Last but not least, the feature extraction process during optimization is introduced to cater to specific operated goal, which confirmed one feasible way of task-oriented structure optimization for mobile painting robot.

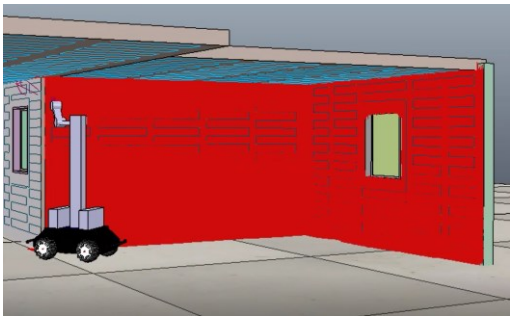

(a) Painting the vertical wall

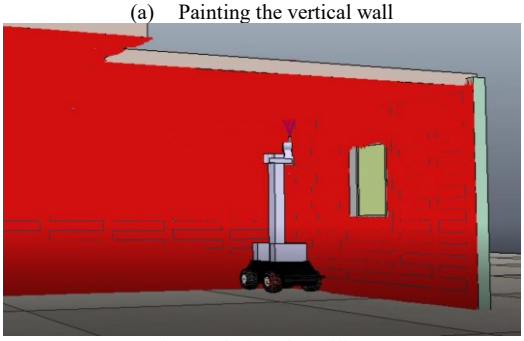

(b) Painting the ceiling

Fig. 8 Simulation-painting the prototype room

TABLE I
PAINTING THICKNESS VERIFICATION

Wall type	Average painting thickness / $\boldsymbol{q}_{d}$	Maximum and minimum painting thickness /$\boldsymbol{q}_{d}$
Vertical wall 1	0.87	1.22/0.78
Vertical wall 2	0.82	1.21/0.79
Vertical wall 3	0.87	1.22/0.77
Vertical wall 4	0.78	1.24/0.78
Vertical wall 5	0.77	1.21/0.78
Ceiling 1	0.94	1.13/0.91
Ceiling 2	0.92	1.12/0.88

IV. CONCLUSIONS

In conclusion, based on the above mentioned contents, it is easy to find that this research mainly focuses on exploring the task-oriented structure parameter optimization for mobile painting robot. To understand the task-oriented optimization process, the detailed expressions for the kinematics of mobile painting robot should be implemented firstly, and then the reachable spatial point for the spray gun can be deduced. Moreover, the designed or optimized structure parameter can guarantee that all the points on the surface will be reached by the spray gun and simultaneously fulfill the given painting requirement. However, the surface painting operation, especially those with irregular shape, means that the infinite target points exist on the operated surface and thereby one "feature point" extraction process is essential to replace the surface with enough finite points during optimization process. Therefore, by taking both the objective and subjective factors into consideration, the key point is about how to search or define these types of feature point and this will be discussed in the future work.

Besides, the solutions obtained via Monte-Carlo algorithm show one huge computing load and tedious calculation process and this is not practical. In order to improve the original optimization process, more advanced algorithm will be tested. As for the painting thickness distribution, the employed painting thickness model is the most typical one and has been widely applied. It is a pity that this model is not accurate when considering the complex experimental factors, such as droplet size, velocity distribution, and the velocity and pressure of gas phase. Therefore, we can conclude that despite the fact that the proposed optimization method can be treated as one feasible way of task-oriented structure optimization for mobile painting robot, but more on-going researches in this field still need to be carried out in the future.

REFERENCES

[1] A. Ehsan, B. Li and I. M. Chen, "A cooperative painting robot for interior finishing of industrial developments," IEEE Robotics & Automation Magazine, vol. 25, no. 2, pp. 82-94, June 2018.

[2] M., Ijeoma W, et al, "Implementation of industrial robot for painting applications," Procedia Engineering, vol. 41, pp. 1329-1335, 2012.

[3] S. M. K. Zaidi, et. al, "Computer aided design of a low-cost painting robot," Mehran University Research Journal of Engineering and Technology, vol. 36, no. 4, pp. 841-856, October 2017.

[4] A. Mayur V and C. Shital S, “Incremental approach for trajectory generation of spray painting robot,” Industrial Robot: An International Journal, vol. 42, no. 3, pp. 228-241, May 2015.
[5] Y. Tang and W. Chen, “Surface modeling of workpiece and tool trajectory planning for spray painting robot,” PLoS ONE, vol. 10, no. 5, pp. e0127139, January 2015.
[6] C. Yan, et al, “Paint thickness simulation for painting robot trajectory planning: a review,” Industrial Robot: An International Journal, vol. 44, no. 5, pp. 629-638, August 2017.
[7] B. Michal, et al, “Mathematical model of the painting robot,” Applied Mechanics and Materials, vol. 843, pp. 72-80, 2016.
[8] M. Zaid, T. S. and A. Selvakumar, A. “Development of exterior wall painting robot,” Indian Journal of Science and Technology, vol. 9, no. 38, October 2016.
[9] C. Ji-Won, et al, “Wind resistance performance analysis of automated exterior wall painting robot for apartment buildings,” KSCE Journal of Civil Engineering, vol. 19, no. 3, pp. 510-519, 2015.
[10] W. Khalil, E. Dombre and M. Nagurka, “Modeling, identification and control of robots,” Applied Mechanics Reviews, vol. 56, no. 3, pp. B37, 2003.
[11] Y. Xu and R. Liu, “Dynamic modeling of SCARA robot based on Udwadia–Kalaba theory,” Advances in Mechanical Engineering, vol. 9, no. 10, October 2017.
[12] R. Paul, “Robot manipulators: mathematics, programming, and control: the computer control of robot manipulators”, MIT Press, Cambridge, MA, 1981.
[13] H. Chen and N. Xi, “Automated robot tool trajectory connection for spray forming process,” Journal of Manufacturing Science and Engineering, vol. 134, no. 2, pp. 021017, 2012.
[14] H. Chen and N. Xi, “Automated tool trajectory planning of industrial robots for painting composite surfaces,” The International Journal of Advanced Manufacturing Technology, vol. 35, no. 7, pp. 680-696, 2008.
[15] H. Chen, et al, “General framework of optimal tool trajectory planning for free-form surfaces in surface manufacturing,” Journal of Manufacturing Science and Engineering, vol. 127, no. 1, pp. 49, 2005.
[16] D. Frenkel, K. Schrenk and S. Martiniani, “Monte Carlo sampling for stochastic weight functions,” Proceedings of the National Academy of Sciences of the United States of America, vol. 114, no. 27, pp. 6924-6929, 2017.